



HAL
open science

The Molecular Basis of the Adsorption of Bacterial Exopolysaccharides on Montmorillonite Mineral Surface.

Lina Henao, Karim Mazeau

► **To cite this version:**

Lina Henao, Karim Mazeau. The Molecular Basis of the Adsorption of Bacterial Exopolysaccharides on Montmorillonite Mineral Surface.. *Molecular Simulation*, 2008, 34 (10-15), pp.1185-1195. 10.1080/08927020802235714 . hal-00515045

HAL Id: hal-00515045

<https://hal.science/hal-00515045>

Submitted on 4 Sep 2010

HAL is a multi-disciplinary open access archive for the deposit and dissemination of scientific research documents, whether they are published or not. The documents may come from teaching and research institutions in France or abroad, or from public or private research centers.

L'archive ouverte pluridisciplinaire **HAL**, est destinée au dépôt et à la diffusion de documents scientifiques de niveau recherche, publiés ou non, émanant des établissements d'enseignement et de recherche français ou étrangers, des laboratoires publics ou privés.

**The Molecular Basis of the Adsorption of Bacterial
Exopolysaccharides on Montmorillonite Mineral Surface.**

Journal:	<i>Molecular Simulation/Journal of Experimental Nanoscience</i>
Manuscript ID:	GMOS-2008-0064.R1
Journal:	Molecular Simulation
Date Submitted by the Author:	14-May-2008
Complete List of Authors:	Mazeau, karim; CNRS, CERMAV Henao, lina; CNRS, CERMAV
Keywords:	molecular modeling, clay, polysaccharide

SCHOLARONE™
Manuscripts

The Molecular Basis of the Adsorption of Bacterial Exopolysaccharides on Montmorillonite Mineral Surface.

Lina Henao and Karim Mazeau

*Centre de Recherches sur les Macromolécules Végétales (CERMAV–CNRS), ICMG FR2607
BP 53, 38041 – Grenoble Cedex 9 – France*

Affiliated with the Joseph Fourier University.

Abstract

Rhizospheric exopolysaccharides (EPS) spontaneously aggregate mineral particles. Molecular dynamics simulations with Cerius2 and Material Studio programs have been performed to study the adsorption of chemical groups, monosaccharides and oligosaccharides, onto the basal surface of Na-montmorillonite. The estimated enthalpies of adsorption of chemical groups nicely reproduced the expected values. Mono- and oligosaccharides have a preferred geometry of adsorption. Monosaccharides maintained their shape upon adsorption whereas oligosaccharides flattened more or less on the surface, depending on their flexibility. The conformational adaptability was shown to be the leading factor that determined the interaction strength between the EPS and the mineral surface.

Introduction

Organic/inorganic hybrid composites are materials that comprise nanometer-size mineral particles dispersed in a polymer matrix. Compared to pure matrix, these materials exhibit enhanced properties : an increase of the mechanical and thermal performances, and a barrier effect to gas diffusion[1, 2]. Most of the matrices considered so far are synthetic polymers; preparing such materials is difficult because of the low compatibility between hydrophobic polymers and the hydrophilic mineral. To overcome this difficulty, the cations located in the interlayer space of the clays are exchanged by tensioactive molecules (principally alkyl ammoniums). The inter layer space thus gain a hydrophobic character and become compatible with polymers.

Such hybrid complexes do exist in nature; rhizospheric microorganisms, i.e. living in the vicinity of plant roots, produce exo-polysaccharides (EPS); these EPS possess two key properties: they aggregate mineral particles[3] and they can retain a large amount of water[4]. The benefit for bacteria is obvious as they are protected by organo-mineral aggregates against

1
2
3 both brutal climatic changes and hydric stress[4-10]. There is also a benefit for the soil, as the
4 presence of aggregates is correlated with soil fertility[11]. Polysaccharides have indeed the
5 additional properties of being biocompatible and biodegradable, two supplementary
6 advantages exploited in an emerging class of biomaterials[12-17].
7

8
9
10 The macroscopic properties reflect the associations occurring at the molecular scale between
11 polysaccharides, mineral particles and water. The surface of montmorillonite for example,
12 bears negative charges; one may intuitively think that the most favorable organic molecules
13 for adsorption onto such mineral are poly-cations. The situation is apparently more
14 complicated as many rhizospheric EPS are shown to interact with minerals[6, 18-24]; they are
15 either neutral or anionic (with one or two charges per repeat unit, generally carboxylic acids).
16 The role of the fine structure of the polysaccharide on its adsorption mechanism onto mineral
17 surfaces remains largely unclear. However, EPS offer a unique opportunity to establish
18 structure-property relationships; their experimental responses to flocculate a colloidal
19 suspension of clays are effectively structure dependant[25, 26] and EPS possess a wide
20 variety of structures: they can be linear or branched. When present, the ionisable group is
21 located either on the backbone or on the side chains (see **figure 1**). To complement the
22 experimental efforts, our objective was thus to reveal, by molecular modeling, the structural
23 factors (if any) of microbial polysaccharides that are responsible for their adsorption on
24 mineral surfaces. Montmorillonite is the chosen mineral; it is widespread on earth, its crystal
25 structure is reported[27] and it is widely studied by molecular modeling (in particular in
26 interactions with organic species)[28-32]. Only the basal surface of montmorillonite was
27 considered in this study as it is statistically the most abundant surface.
28
29
30
31
32
33
34
35
36
37
38
39
40
41
42

43 **Material and Methods.**

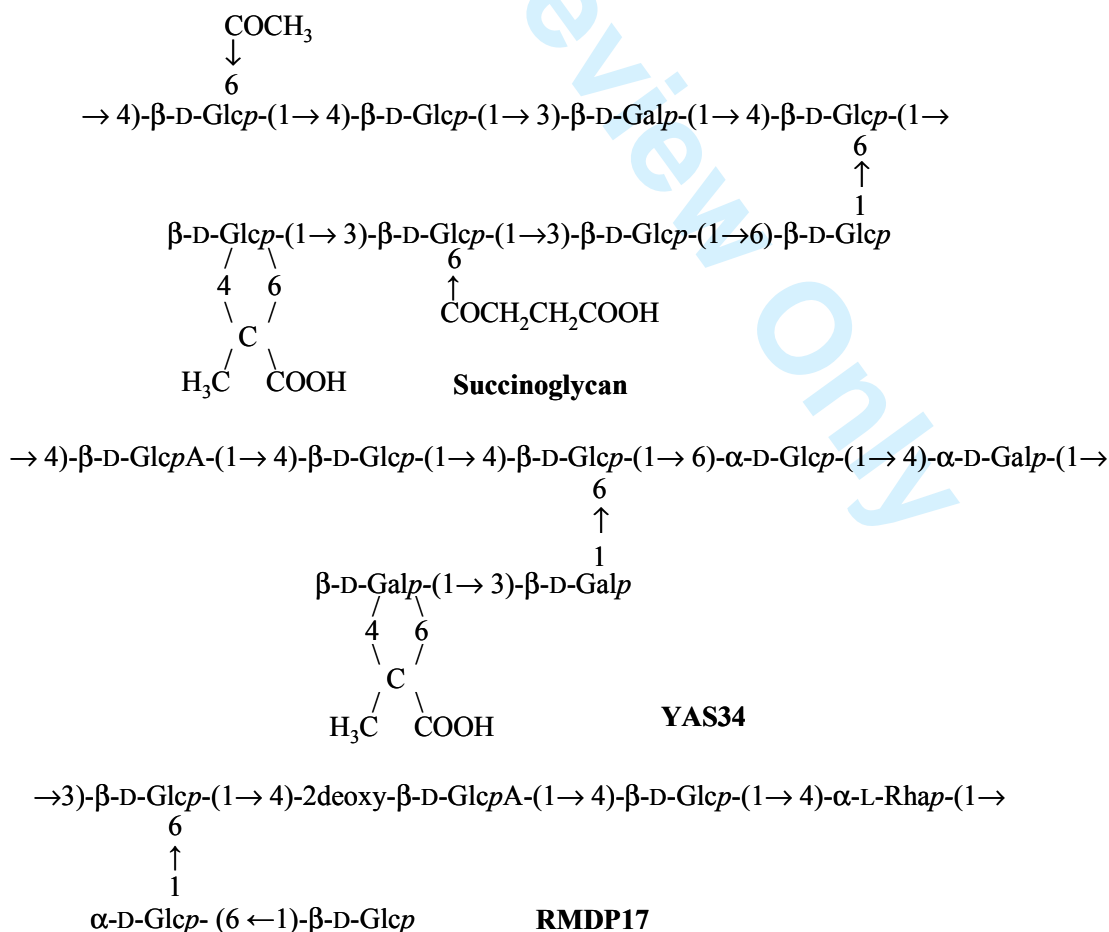
44
45 In this study, we have used the modeling softwares Cerius² and Material studio (accelrys inc.)
46 running on silicon graphics workstations at the Centre d'Expérimentation et de Calcul
47 Intensif, CECIC, Grenoble, France.
48
49
50
51
52

53 **Construction of the initial structures.**

54 *Mineral surface.*

55
56 Montmorillonite is a smectite type mineral clay, it is a hydrophilic mineral that consists of a
57 nanometer-thick layers formed by sandwiching an aluminum octahedron sheet between two
58 silicon tetrahedron sheets. The initial unit cell was built from relevant crystallographic
59 coordinates of a pyrophyllite crystal, published by Tsipursky and Drits[27], using the Crystal
60

Builder modulus. The experimental lattice is monoclinic, with space group C2/m, and the lattice parameters: $a=5.20$, $b=9.20$, $c=10.13$ and $\alpha=90^\circ$, $\beta=99^\circ$, $\gamma=90^\circ$. The unit cell is duplicated along the two directions parallel to the sheet planes. Then, we performed substitution of some Al^{3+} by Mg^{2+} in the octahedral layer and substitution of some Si^{4+} atoms by Al^{3+} in the tetrahedral layer in order to obtain the desired final chemical composition of the Wyoming Na-montmorillonite : $\text{Na}_{0.75}(\text{Si}_{7.75}\text{Al}_{0.25})(\text{Al}_{3.5}\text{Mg}_{0.5})\text{O}_{20}(\text{OH})_4$. This structure has a cation exchange capacity (CEC) of 1.01 meq/g; the CEC is defined as the amount of the exchangeable cations retained by the clay to neutralize the negative charge (milliequivalent of positive charge per gram of clay). Periodic boundary conditions are applied in all the three dimensions. Typical a , b dimensions of the periodic cell are $17.8 \text{ \AA} \times 30.4 \text{ \AA}$, corresponding to a surface area of 5.4 nm^2 . This surface was used to study the adsorption of small molecules (chemical functions and monosaccharides). A larger surface was also built to model the adsorption of the largest structures (oligomers). Cell parameters of the large surface model were $72.8 \text{ \AA} \times 62.1 \text{ \AA}$, (area of 45 nm^2). The clay mineral is then minimized, equilibrated by molecular dynamics (NPT at 300 K and 1 atm) and then optimized again. To generate a mineral surface convenient for the simulation, the lattice constant c of the cell was extended to 100 \AA . Surfaces were then hydrated by a monolayer of water molecules.



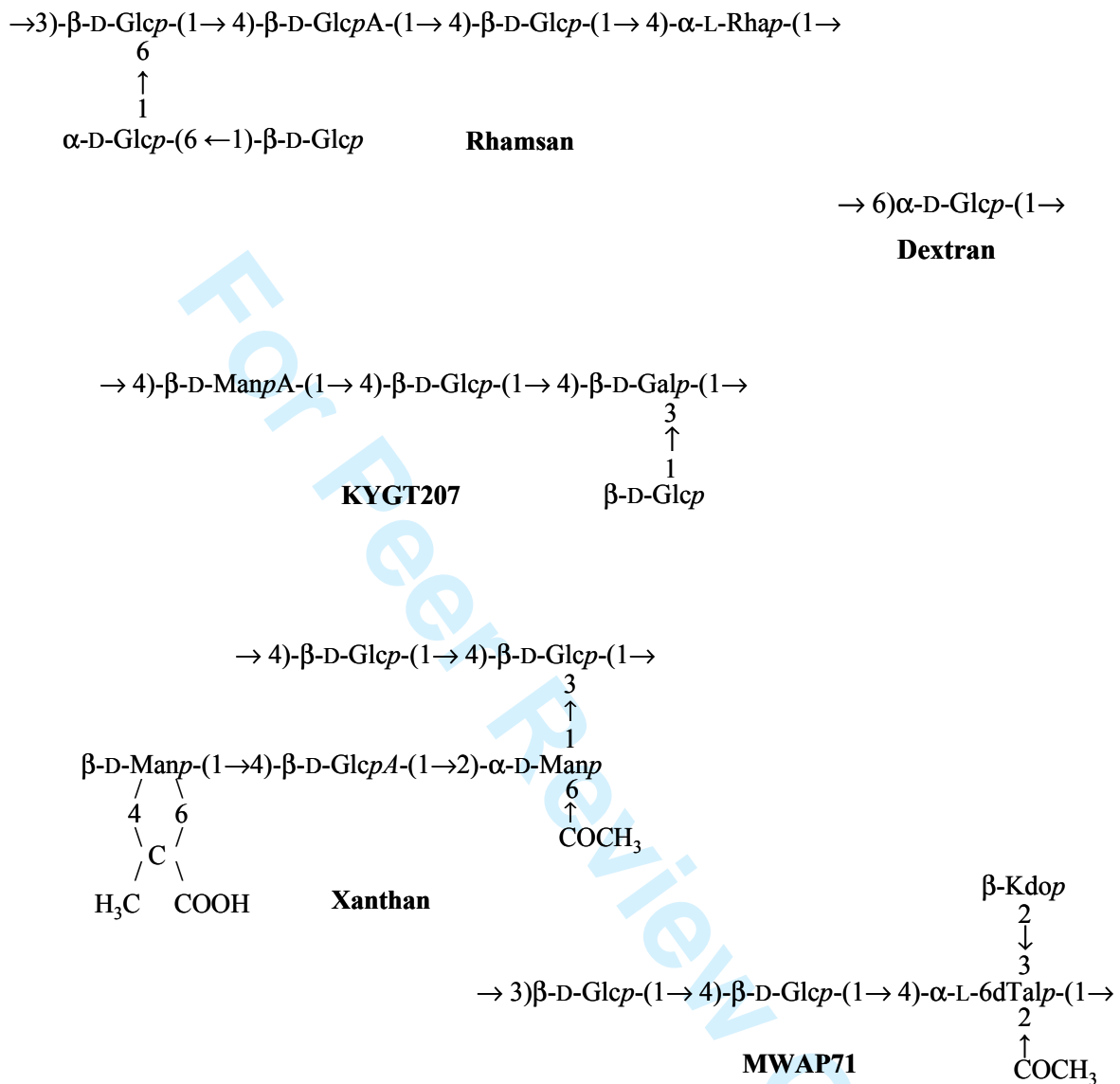


Figure 1. Chemical structures of the polysaccharides considered in this study.

Organic chemicals.

We studied the adsorption of chemical groups, monosaccharides and oligosaccharides; they are all related to the EPS indicated in **Figure 1**. The chemical groups considered are : methane (CH_4), ethane (CH_3CH_3), methanol (CH_3OH), ethanol ($\text{CH}_3\text{CH}_2\text{OH}$), 2-propanol ($\text{CH}_3\text{CH}_2\text{OHCH}_3$), methanoic acid (HCOOH), ethanoic acid (CH_3COOH), methanal (HCHO), ethanal (CH_3CHO), dimethyl ketone ($\text{CH}_3(\text{CO})\text{CH}_3$), methoxymethane (CH_3OCH_3), methyl ethanoate ($\text{CH}_3(\text{CO})\text{OCH}_3$), sodium acetate ($\text{CH}_3\text{COO}^-\text{Na}^+$). The twenty monosaccharides

1
2
3 considered are indicated in **Table 2**; the two hydroxyl groups involved in glycosidic bonds
4 have been systematically changed to OMe groups.

5
6
7 The oligomers considered in this part correspond to a unique repeat unit of selected EPS
8 synthesized by rhizospheric microbes: dextran, MWAP71, RMDP17, Rhamsan, xanthan,
9 YAS34 and succinoglycan; their primary structures are reported in **Figure 1**. A degree of
10 polymerisation of 6 was chosen for the dextran to obtain a molar mass comparable to the
11 other oligomers (see **Table 4**). Polysaccharides are usually highly polydispersed; dextran for
12 example represents a family of homopolysaccharides that feature a substantial number of
13 consecutive α -(1 \rightarrow 6) linkages in their main chain, usually more than 50% of the total
14 linkages. Dextrans also possess variable amount of side chains constituted by mono and/or
15 oligosaccharides linked to the main chain by (1 \rightarrow 3) and (1 \rightarrow 2) linkages. It is obviously not
16 possible to consider all the possible chemical structures for a given polysaccharide so that
17 each model correspond only an idealized structure; consequently, the dextran modelled in our
18 study is only represented by its dominant structural feature (see Figure 1). In addition, some
19 of the polysaccharides are known to form multiple helices in solution (xanthan for example);
20 only the simple chain was considered in our study.

21
22
23 Chemical groups, monosaccharides and repeat units of EPS were constructed from standard
24 geometries of bond lengths and bond angles, thanks to the sketcher module. The initial
25 conformation of the pyran ring of monosaccharides is 4C_1 for Glc, Man, Gal and Kdo
26 residues, or 1C_4 for Rha and Tal. In the case of oligosaccharides, values of the conformational
27 parameters describing the relative orientation of two consecutive monomers (torsion angles
28 Φ , Ψ and ω) were derived from the conformational analysis of model disaccharides[33 , 34].
29 Torsion angle values correspond to the lowest energy minimum and/or auxiliary minima of
30 the (Φ , Ψ) potential energy surfaces. Explicit hydrogen atoms were used in all model systems.
31 Each structure was then relaxed to minimize energy and avoid atom overlaps.

32 33 34 35 36 37 38 39 40 41 42 43 44 45 46 47 48 49 50 51 52 53 54 55 56 57 58 59 60 *Modelling the adsorption.*

An organic molecule is then inserted in the simulation box above the mineral surface in a
random orientation. Configurational sampling was then performed using a combination of
energy minimization and molecular dynamics at elevated temperatures, typically 400 to 600
K. A typical dynamic simulation lasts 500 ps for the shortest ones, up to 2 ns for the longest
ones. Once adsorbed, a 20Å slab of amorphous water molecules was added to the system. The
resulting hydrated model was first minimized, equilibrated for 10 ps and minimized again

1
2
3 prior to analysis. Calculations have been repeated three times on several test cases, results
4 were consistent.
5
6

7 8 *Computational details.*

9
10 The Universal force field was used, UFF[35]. This choice resulted from a compromise
11 between good accuracy and availability of the parameters for all atom types present in the
12 molecular models. This force field was successfully used in independent studies of organo-
13 clay species[29, 36, 37: Pospisil, 2004 #54]. Furthermore, preliminary tests reveal that this
14 force field correctly reproduces the particular conformational properties of carbohydrates:
15 puckering of the pyran rings and the exo-anomeric effect. The charge equilibration method
16 was used to calculate charges for each atom[38]. Long-range interactions were treated by the
17 Ewald summation technique[39]. The simple point charge model (SPC) was used for the
18 water molecules.
19

20 The minimization uses the conjugate gradient procedure with the convergence criterion of the
21 root-mean-square of the atomic derivatives of $0.05 \text{ kcal mol}^{-1} \text{ \AA}^{-1}$.
22

23 Molecular dynamic calculations were based on the canonical NVT ensemble (constant
24 number of particles, volume, and temperature). The equations of motion were solved using
25 the standard Verlet algorithm[40], with a time step of 1 fs. The system is coupled to a bath at
26 the desired temperature using Nose's algorithm[41]. During the production MD simulations,
27 the positions of the mineral surface atoms were fixed, but all remaining system components
28 (counter ion, organic molecule, water) were allowed to move accordingly.
29

30 31 *Properties.*

32 33 Enthalpies of adsorption.

34 Ten structures (snapshots) were randomly selected and minimized from the molecular
35 dynamic trajectory. The total potential energy of a microstate may be written as:
36
37

$$38 \quad E_{\text{tot}} = E_{\text{clay}} + E_{\text{ligand}} + E_{\text{inter}}$$

39 where the first three terms represent the energy of the total system, the energy of
40 montmorillonite alone, and the energy of the ligand molecule, and consist of both valence and
41 nonbonded components. The last term is the interaction energies between the clay and the
42 ligand (consisting of nonbonded terms only). The enthalpy of adsorption is taken as the
43 negative of the interaction energies of the 10 selected structures:
44
45
46
47
48
49
50
51
52
53
54
55
56
57
58
59
60

$$\Delta H_{\text{ads}} = -\langle E_{\text{inter}} \rangle$$

We were interested by the energy change of the carbohydrate structure when it goes out of the solution to the adsorbed state : ΔE . Dynamic trajectories of the carbohydrate structures were thus performed, in the absence of the mineral surface.

$$\Delta E = E_{\text{ads}} - E_{\text{Free}}$$

where E_{ads} and E_{Free} are the energies of the adsorbed and isolated (in the absence of the mineral surface) conformations, respectively.

Surface area in contact.

The estimation of the molecular surface areas was performed with the Connolly dot algorithm,[42] with a probe radius of 1.4 Å.

Hydrogen bonds.

The method traditionally used to detect a hydrogen bond is geometric: two oxygen atoms are considered hydrogen bonded if the distance between the hydrogen of the donor and the oxygen acceptor is lower than 2.5 Å and if the angle between the oxygen donor, the hydrogen donor and the oxygen acceptor larger than 90°.

Results and discussion.

A hierarchical approach was chosen to reveal the adsorption behavior of polysaccharides onto the basal surface of the clay mineral. Adsorption of chemical groups was examined first, followed by adsorption of monosaccharides. Finally the adsorption of oligosaccharides was considered. **Idealized** chemical structures of the EPS are given in **Figure 1**; it was experimentally shown that all of them do adsorb on mineral surfaces. Predicted quantities are the energies associated with the binding and also the geometry of the complexes.

During the dynamics trajectory, the total energy decreases when the saccharide adsorbs onto the surface of the clay mineral, suggesting that the whole modeled system reaches a more stable state. Consequently, the positive values of ΔH_{ads} (or the negative values of E_{int}) indicate that the adsorption is a favorable process.

Adsorption of functional groups.

During the dynamics simulation, the chemical groups explore several adsorption sites of similar energy. **Table 1** gives their average interaction energies with the mineral surface. The counter ion has no noticeable effect on the interaction of hydrophobic groups (Methyl and Ethyl) with the clay surface. In contrast, it strongly participates to the interaction with polar groups. Alcohol and carboxyl groups form Hydrogen Bonds with the oxygen atoms of the mineral surface; electrostatic interactions (ionic like) also occur, between the oxygen atoms of the organic molecule and the counter ion.

The interaction of very small molecular fragments of saccharides with the mineral surface can be considered unperturbed by structural effects, the interaction is thus optimal and the estimated values of the enthalpies of adsorption give the orders of magnitude of the energies involved upon adsorption. The interaction of the different functions on the mineral surface is globally weak; the energy of a hydrogen bond O-H...O and a hydrophobic interaction are typically in the range 4 to 5 kcal/mol and 1 to 3 kcal/mol, respectively. Our results are in agreement with these values, suggesting that the force field correctly reproduces the basic interaction energies.

Group	Without counter-ion				With counter-ion			
	E_c	E_{vw}	E_{tot}	S_{int}	E_c	E_{vw}	E_{tot}	S_{int}
CH ₄	0	-6	-6	18	-1	-6	-7	18
CH ₃ OH	-3	-7	-10	22	-28	-3	-31	24
HCHO	-5	-6	-11	16	-21	-4	-25	23
HCOOH	-1	-7	-8	22	-17	-5	-22	23
CH ₃ CH ₃	0	-9	-9	25	-4	-8	-12	25
CH ₃ CH ₂ OH	-2	-11	-13	27	-30	-5	-35	28
CH ₃ CHO	-5	-10	-15	22	-23	-8	-31	28
CH ₃ COOH	-1	-11	-12	30	-20	-8	-28	30
CH ₃ OCH ₃	0	-11	-11	34	-31	-6	-37	32
CH ₃ CHOHCH ₃	-2	-13	-15	30	-29	-8	-37	30
CH ₃ (CO)CH ₃	-2	-13	-15	35	-25	-10	-35	34
CH ₃ (CO)OCH ₃	-2	-14	-16	36	-29	-12	-41	41

Table 1. Energies (kcal/mol) and interacting areas (\AA^2) of several chemical moieties adsorbed onto the mineral surface. E_{tot} : total energy, E_c and E_{vw} are its coulomb and Van der Waals components. Standard deviations on energies ranged between 1 to 3 kcal/mol and those on surfaces ranged between 1 to 5 \AA^2 .

Monosaccharides and oligosaccharides

Monomer	Substituents	S_{tot}	Without counter-ion			With counter-ion		
			E_{int}	S_{int}	ΔE	E_{int}	S_{int}	ΔE
β -D-Glcp	Me1	192	-31	69	4	-99	81	13
β -D-Glcp	Me1, Me3	205	-35	84	2	-107	93	12
β -D-Glcp	Me1, Me4	203	-34	83	7	-104	85	15
β -D-Glcp	Me1, Me3, Me4	222	-39	87	6	-111	102	15
β -D-Glcp	Me1, Me4, Me6	220	-43	93	8	-123	98	19
β -D-Glcp	Me1, Me6	209	-38	83	-3	-113	92	12
α -D-Glcp	Me1, Me6	209	-33	76	6	-120	87	17
β -D-Glcp	Me1, Me4, 6-COCH ₃	253	-43	94	1	-110	104	10
β -D-Glcp	Me1, Me3, 6-COCH ₂ CH ₂ COOH	307	-48	116	13	-146	129	26
β -D-GlcpA	Me1, Me4	208	-34	82	-3	-88	82	6
2deoxy- β -D-GlcpA	Me1, Me4	199	-36	83	-2	-95	93	19
β -D-Glcp	Me1, 4-6pyruvate	239	-35	86	0	-84	84	4
β -D-Galp	Me 1, Me 3	209	-35	79	3	-94	81	7
α -D-Galp	Me 1, Me 4	202	-32	68	-3	-90	77	12
β -D-Galp	Me 1, 4-6pyruvate	235	-31	81	8	-97	90	15
α -D-Manp	Me 1, Me 2, 6COCH ₃	241	-36	82	5	-95	96	17
β -D-Manp	Me 1, 4-6pyruvate	235	-31	81	-1	-92	91	2
α -L-Rhap	Me 1, Me 4	193	-25	58	1	-53	62	3
β -Kdop	Me2	225	-30	72	4	-106	77	14
α -L-6dTalp	Me1, Me3, Me4, 2COCH ₃	242	-24	58	4	-92	74	14

Note: Kdo is the 3-deoxy-D-Manno-oct-2-ulosonic acid.

Table 2. Energetic and geometric characteristics of selected monomers of carbohydrates adsorbed onto the clay mineral surface in the presence or absence of counter-ion. Energy of interaction (E_{int} in kcal/mol); difference in energy between the free state and the adsorbed state (ΔE in kcal/mol). Total solvent exposed surface (S_{tot} in \AA^2), surface in interaction (S_{int} in

1
2
3 \AA^2). Standard deviations on energies ranged between 2 to 8 kcal/mol and those on surfaces
4 ranged between 1 to 14 \AA^2 .
5
6
7

8
9 Dynamical behavior of mono- and oligosaccharides differ from that of functional groups.
10 They touched the mineral surface and explored several orientations prior to converging to
11 their preferred adsorption geometry. This suggests that the potential energy surface has many
12 energy minima. The energy decreases gradually with time during the course of the simulation
13 and only the final parts of the trajectories were considered (when the total energy is stabilized
14 to its minimal value), in order to estimate the interaction energies. On average, only 30 to
15 40% of the total accessible surface of monosaccharides is in direct contact with the mineral
16 surface; this value is remarkably unchanged for the oligomeric fragments.
17
18
19
20
21
22
23

24 **Monosaccharides.**

25
26 All the monomers considered in this study are indicated in **Table 2** with the structural and
27 energy details of their adsorption on the mineral surface.
28

29
30 The adsorption enthalpy strongly depends on several factors, including the number of pendant
31 groups, their nature, position and orientation with respect to the pyran ring. **Figure 2**
32 compares the preferred geometry of interaction of two glucoses 1,6 dimethylated (α and β).
33 Inverting the configuration on the anomeric carbon atom changed the adsorption features of
34 the monosaccharide on the mineral surface.
35
36
37

38
39 Here again, the counter ion favors the adsorption of the monosaccharides. The average
40 interaction energy was -30 kcal/mol in the absence of counter ions; it reached -106 kcal/mol
41 in their presence. Inspection of the models reveals the strong similarity of the binding of
42 monosaccharides with that of the functional groups: hydrogen bonds and ionic interactions.
43 Hydrophobic interactions seem to play a particular role. Methyl groups were in direct contact
44 with the surface and the monosaccharide-surface interaction was stronger when more O-
45 methoxy groups were present (see Table 2).
46
47
48
49
50
51
52
53
54
55
56
57
58
59
60

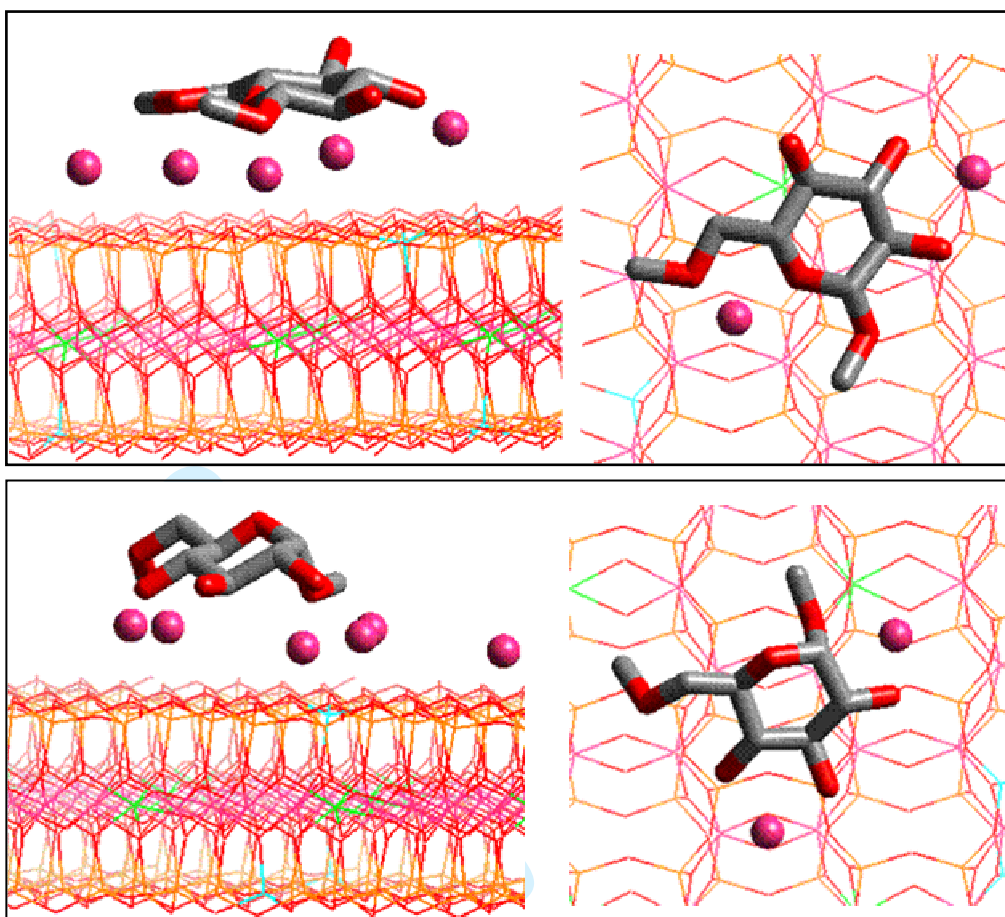


Figure 2. Equilibrium adsorbed geometry of β -glucose (top) and α -glucose (bottom) methylated at positions 1 and 6. Left side views, right front views. Hydrogen atoms are omitted for clarity.

The group contribution method clearly overestimated the interaction energies. For example, group method predicts an energy of interaction of about -200 kcal/mol for a simple di-substituted Glucose molecule. The energies really involved with the adsorption of such molecules are much lower than this expected value, they ranged between -104 kcal/mol and -120 kcal/mol. This is not surprising as the group contribution assumes an optimal interaction whereas, in reality, the adsorption is far from perfect. In addition, structural effects are neglected in the group method; it cannot discriminate between different stereo isomers.

The changes in the conformational energies (ΔE) were minimal for the monosaccharides. They are made of a pyran ring which adopts a dominant chair conformation, except for very rare cases. The chair geometry remained when the monosaccharide is adsorbed, by contrast, side chains showed flexibility.

Oligomers : repeat units of EPS.

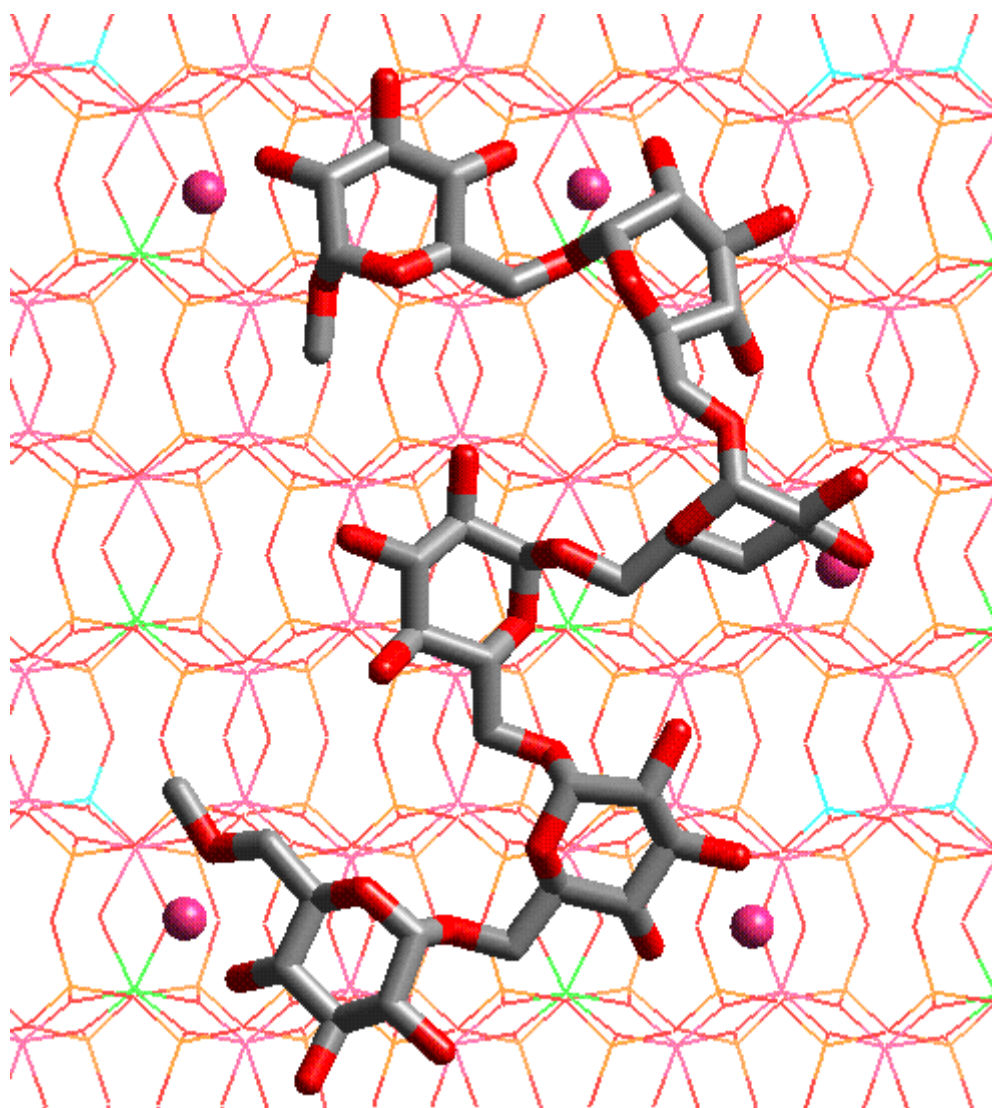
Given the results of the previous section, simulations on the oligomeric structures of carbohydrates were systematically performed in the presence of the counter ions. Their energies of interaction with the clay surface are given in **Table 3**, the geometrical aspects of the adsorption are given in Table 4.

	ΔH_{Ads}	E_{adsorb}	E_{Free}	RMSD
dextran	351	725	646	0,0234
KYGT207	240	486	442	0,0304
MWAP71	151	421	394	0,0145
rhamsan	333	686	615	0,0362
RMDP17	316	603	509	0,0465
succinoglycan	564	950	785	0,0245
xanthan	268	592	541	0,0230
YAS34	445	958	841	0,0153

Table 3. Selected characteristics of the repeat units of EPS. ΔH_{Ads} : enthalpy of adsorption of the oligomer on the mineral surface, E_{adsorb} : average energy of the adsorbed conformation, E_{Free} : average energy of the equilibrium conformation in the absence of the surface, RMSD root mean square deviation per atom between the free and the adsorbed conformations. Energies are given in kcal/mol.

	S_{totcompl}	S_{Free}	S_{interact}	Mw
dextran	806	743	345	1018
KYGT207	550	531	239	708
MWAP71	599	595	202	778
rhamsan	796	737	340	1016
RMDP17	802	745	314	1000
succinoglycan	1244	1071	549	1554
xanthan	773	735	304	982
YAS34	942	967	386	1264

1
2
3 Table 4. Geometric characteristics (in \AA^2) of the adsorption of the repeat units of EPS.
4
5 S_{totcomp1} : solvent accessible surface of the adsorbed conformation, S_{Free} solvent accessible
6 surface of the free conformation, S_{interact} area in interaction. Molecular masses of the different
7 fragments of EPS are also indicated (Mw).
8
9



48 Figure 3. Equilibrium adsorbed geometry of the dextran fragment. Hydrogen atoms and water
49 molecules are omitted for clarity.
50

51
52
53 Inspecting the molecular models shows that the monomers in the adsorbed conformational
54 state do not systematically adopt the unperturbed orientation revealed in the preceding
55 section. To illustrate this, **Figure 3** gives the adsorbed fragment of dextran ; among its six α -
56 Glc residues ; four of them adsorb in an identical geometry already observed in the study of
57 free monosaccharides ; by contrast, the remaining two α -Glc behave differently. Chemical
58
59
60

connectivity induces geometrical constraints that limit the number of accessible orientations of the constituent monosaccharides with respect to the mineral surface. However, the potential energy surface contains a huge amount of energy minima; monomer units that are part of a polymer simply explore secondary potential wells.

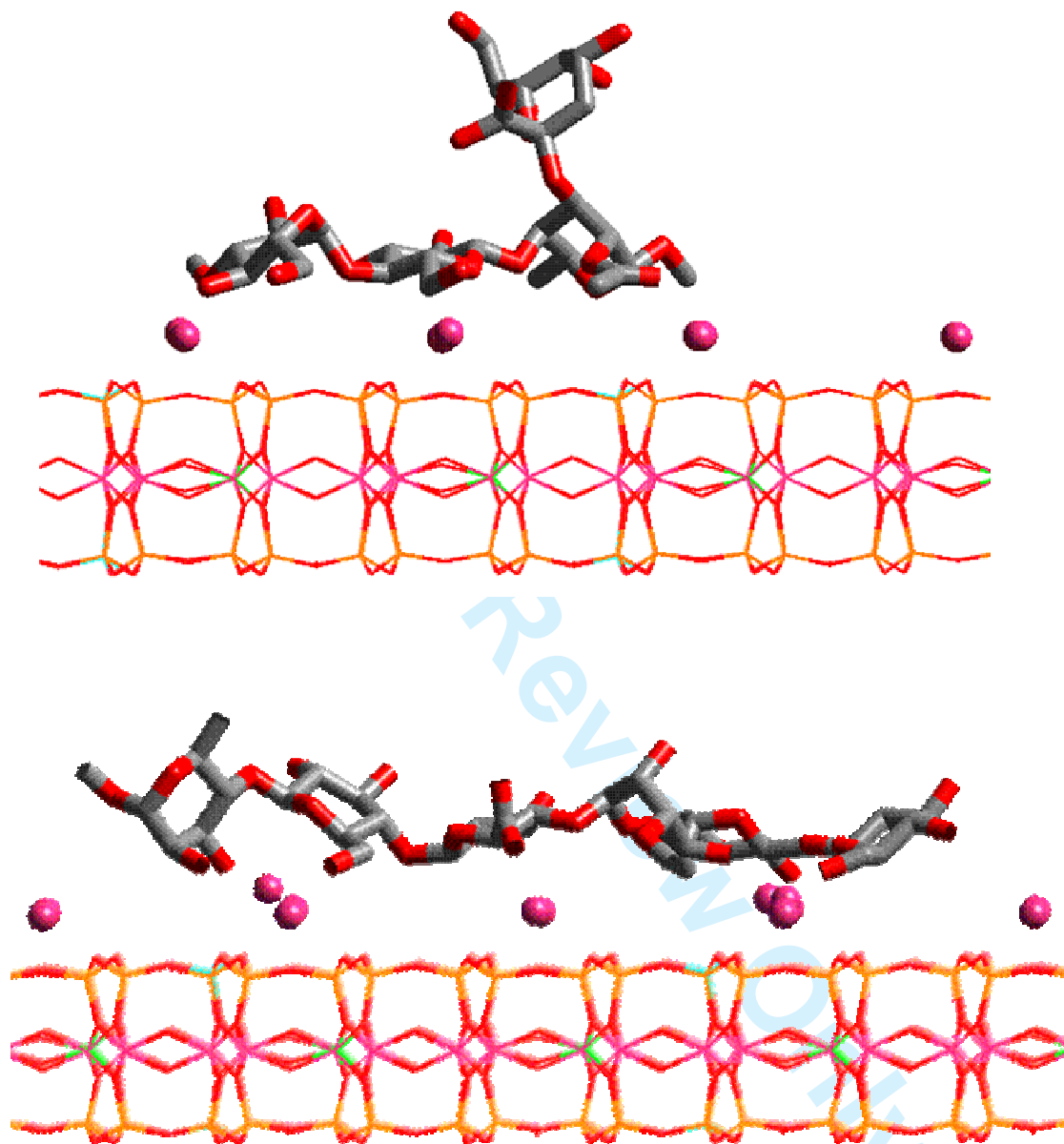


Figure 4. Equilibrium adsorbed geometry of the MWAP71 (top) and the RMDP17 (bottom).

Hydrogen atoms and water molecules are omitted for clarity.

The presence of the surface systematically induced an increase of the internal energy of the EPS fragments. The conformation was thus less stable when adsorbed than when isolated; the difference reaches 20% in the case of RMDP17 and succinoglycan. The presence of the surface also induced an increase of the total accessible surface of the organic molecule. The

oligosaccharides unfolded and thus maximized the contact area with the mineral surface. Figures 3 and 4 show the repeat units of MWAP71 and RMDP17 adsorbed on the surface. The RMDP17 oligosaccharide flattened on the surface, all the monomer units were in direct contact with the surface (**Figure 4**). On the other hand the pendent monomer Kdo (which bears the carboxylic group) of MWAP71 was not in contact with the clay. RMSD compares coordinates of the conformation when adsorbed with the free conformation; it indicates the extent of modification of the shape of the sugar with adsorption. RMSD strongly vary from one EPS to the other; it reached 17% for succinoglycan and it was minimal for the MWAP71 and YAS34.

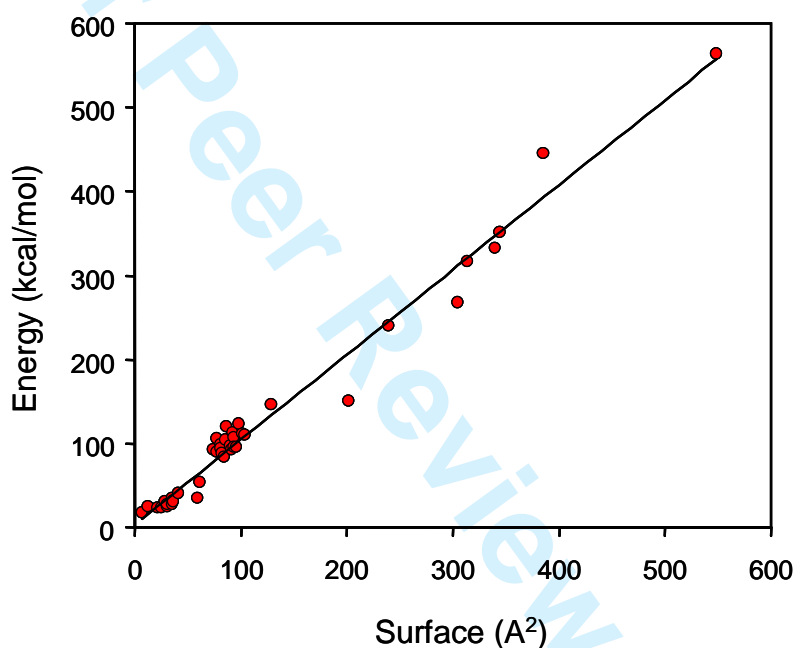


Figure 5. Energy of adsorption as a function of the interacting area.

Figure 5 gives the correlation between the estimated enthalpies of adsorption and the effective interacting area. The linear relationship suggests that the real area in interaction is the critical factor on which depends the adsorption of the tested EPS. Structural factors play a role in the deviation with respect to the master line.

All these results strongly suggest that the oligosaccharide have one (or several) unperturbed solution conformation and another conformation when it is adsorbed on a surface. In contrast with the rigid monosaccharides, the glycosidic bonds linking the monomers together provide conformational freedom in an oligomeric structure. Such flexibility allows the oligomer to

1
2
3 change its shape upon interaction with the mineral surface. In other words, the more flexible
4 the structure, the stronger the interaction. It is thus obvious that the deformation ability (to
5 optimize the interaction) of linear polymers is larger than that of branched polymers for which
6 the side chains induce a steric hindrance that restrict the flexibility of the whole molecule.
7 Accordingly, the fragment of MWAP71 (**Figure 4**) is rigid; its conformational adaptation is
8 restricted to 3 glycosidic bonds and the Kdo pendant group is not in interaction with the
9 surface. In contrast the large flexibility of RMDP17 (5 glycosidic bonds) allows all its
10 monomer units being in contact with the surface.
11
12
13
14
15
16
17
18

19 **Comparison with the experiments.**

20 The accuracy of the models could be assessed by comparing the predicted data to the
21 experimental data. Our results revealed the strong participation of the counter ion in the
22 stability of the complex. They considerably increased the interaction energy between the EPS
23 segment and the mineral surface. The crucial role of electrostatic (ionic) interactions through
24 counter ions is also revealed by many experiments[22, 43-45]. Complexes were also
25 stabilized by hydrogen bonds and hydrophobic interactions. Experimental data show that
26 adsorption of ethyl(hydroxyethyl)cellulose on talc is destabilized by urea, which is an
27 hydrogen bond breaker[12]. Finally, the importance of the hydrophobic interactions is counter
28 intuitive; it is however consistent with NMR results which indicate that aliphatic chains are in
29 direct contact with montmorillonite[46]. Our models also showed that the oligosaccharides
30 undergo conformational changes between the solution states and the adsorbed state. Quartz
31 crystal microbalance with dissipation monitoring (QCM-D) experiments reveal that the
32 adsorbed conformation of dextran on alumina differs from that in solution[47].
33
34
35
36
37
38
39
40
41
42
43

44 Experiments are also performed to establish the structure-property relationships. The ability
45 of several EPS to flocculate a colloidal suspension of clay particles is compared[26].
46 Experiments measure the average size of the flocs which indirectly reflects the efficiency of
47 the EPS to bridge different mineral particles. Such measurements thus give an indication of
48 the affinity of the EPS with the mineral surface. An interaction efficiency coefficient (IEC)
49 was defined in order to allow the comparison between the experimental and modeling
50 approaches. The IEC corresponded to the enthalpy of adsorption, normalized by the effective
51 interaction area. Experimental floc size in the presence of succinoglycan (335 μm) is much
52 larger than that of xanthan (158 μm); even though the molar mass of the xanthan sample is
53 twice the mass of succinoglycan. In qualitative agreement with the experiments, IEC of
54 succinoglycan (1027 $\text{cal/mol}\text{\AA}^2$) was estimated larger than that of xanthan (882 $\text{cal/mol}\text{\AA}^2$).
55
56
57
58
59
60

1
2
3 The molecular masses of dextran and YAS34 are identical ($2 \cdot 10^6 \text{ g}\cdot\text{mol}^{-1}$), their floc sizes are
4 140 and 213 μm , respectively. YAS34 is thus much more efficient than dextran with respect
5 to flocculation ability. Estimated IEC reproduced the experimental tendency: they were
6 estimated at 1017 and 1152 $\text{cal}/\text{mol}\text{\AA}^2$ for dextran and YAS34, respectively.

7
8
9
10 Quantitative comparison between experimental data and the present modeling results is not
11 possible because of both experimental difficulties and assumptions in modeling. Molar
12 masses of the different polysaccharides studied experimentally differ by almost a factor of 20;
13 it is well recognized that such characteristics strongly impact on polymer adsorption on
14 surfaces. In addition, modeling is performed on idealized chemical structures of the EPS and
15 the analysis of the results was based only on the enthalpies of adsorption. The free energy of
16 adsorption would be the choice parameter but the entropic contribution is hardly accessible.
17 The entropy depends on two major contributions: de-solvation of the surfaces, which is a
18 favorable process, and the conformational restrictions of the polymer upon adsorption; which
19 gives non-favorable entropy.
20
21
22
23
24
25
26
27
28
29

30 **Conclusion.**

31 Atomic level molecular simulations were applied to investigate the interaction features of
32 model molecules mimicking bacterial exopolysaccharides (in their neutral forms) with the
33 basal surface of Na-montmorillonite surface. The study has been performed using Cerius2 and
34 material studio modeling programs.

35
36
37
38 It was found that hydrogen bonds, electrostatic and hydrophobic interactions are present in the
39 model systems and provide a significant effect on the adsorption strength of EPS fragments
40 on the mineral surface. The adsorption of monosaccharides was dependant on the nature of
41 the monomer and its side chains. The six-membered ring stayed in its preferred geometry
42 when adsorbed. In contrast, oligosaccharides changed their shape upon adsorption. It was
43 found that the enthalpies of adsorption linearly increase with increasing the interacting surface
44 area, suggesting that the key factor determining the adsorption is the ability of the EPS to
45 unfold in order to maximize its surface in contact. The most flexible structures were the most
46 favorable candidates for adsorption. The present modelling was able to predict a complex
47 physical adsorption phenomenon in agreement with the experimental results.
48
49
50
51
52
53
54
55
56
57

58 **References**

59 [1] S. S. Ray, M. Okamoto. Polymer/layered silicate nanocomposites: a review from
60 preparation to processing. *Progress in Polymer Science*. **28**,1539 (2003).

- 1
2
3 [2] M. Alexandre, P. Dubois. Polymer-layered silicate nanocomposites: preparation,
4 properties and uses of a new class of materials. *Materials Science & Engineering, R: Reports*.
5 **R28**,1 (2000).
6
7
8 [3] J. M. Dorioz, M. Robert, C. Chenu. The role of roots, fungi and bacteria on clay particle
9 organization. An experimental approach. *Geoderma*. **56**,179 (1993).
10
11 [4] C. Chenu. Clay- or sand-polysaccharide associations as models for the interface between
12 microorganisms and soil: water related properties and microstructure. *Geoderma*. **56**,143
13 (1993).
14
15 [5] E. B. Roberson, M. K. Firestone. Relationship between desiccation and exopolysaccharide
16 production in a soil *Pseudomonas* sp. *Applied and Environmental Microbiology*. **58**,1284
17 (1992).
18
19 [6] Y. Alami, W. Achouak, C. Marol, T. Heulin. Rhizosphere soil aggregation and plant
20 growth promotion of sunflowers by an exopolysaccharide-producing *Rhizobium* sp. strain
21 isolated from sunflower roots. *Applied and Environmental Microbiology*. **66**,3393 (2000).
22
23 [7] M. Ashraf, S. Hasnain, O. Berge, T. Mahmood. Inoculating wheat seedlings with
24 exopolysaccharide-producing bacteria restricts sodium uptake and stimulates plant growth
25 under salt stress. *Biology and Fertility of Soils*. **40**,157 (2004).
26
27 [8] P. G. Hartel, M. Alexander. Role of extracellular polysaccharide production and clays in
28 the desiccation tolerance of cowpea bradyrhizobia. *Soil Science Society of America Journal*.
29 **50**,1193 (1986).
30
31 [9] C. Chenu, Y. Le Bissonnais, D. Arrouays. Organic matter influence on clay wettability
32 and soil aggregate stability. *Soil Science Society of America Journal*. **64**,1479 (2000).
33
34 [10] D. Cosentino, C. Chenu, Y. Le Bissonnais. Aggregate stability and microbial community
35 dynamics under drying-wetting cycles in a silt loam soil. *Soil Biology & Biochemistry*.
36 **38**,2053 (2006).
37
38 [11] C. Chenu, J. Guerif, A. M. Jaunet. Polymer bridging: A mechanism of clay and soil
39 structure stabilization by polysaccharides. *Transactions, World Congress of Soil Science*,
40 *15th, Acapulco, Mexico, July 10-16, 1994*. **3a**,403 (1994).
41
42 [12] S. Simon, D. Le Cerf, L. Picton, G. Muller. Adsorption of cellulose derivatives onto
43 montmorillonite: a SEC-MALLS study of molar masses influence. *Colloids and Surfaces, A:*
44 *Physicochemical and Engineering Aspects*. **203**,77 (2002).
45
46 [13] H.-M. Park, M. Misra, L. T. Drzal, A. K. Mohanty. "Green" Nanocomposites from
47 Cellulose Acetate Bioplastic and Clay: Effect of Eco-Friendly Triethyl Citrate Plasticizer.
48 *Biomacromolecules*. **5**,2281 (2004).
49
50
51
52
53
54
55
56
57
58
59
60

- 1
2
3 [14] H.-M. Park, A. K. Mohanty, L. T. Drzal, E. Lee, D. F. Mielewski, M. Misra. Effect of
4 Sequential Mixing and Compounding Conditions on Cellulose Acetate/Layered Silicate
5 Nanocomposites. *Journal of Polymers and the Environment*. **14**,27 (2006).
6
7
8 [15] S. F. Wang, L. Shen, Y. J. Tong, L. Chen, I. Y. Phang, P. Q. Lim, T. X. Liu. Biopolymer
9 chitosan/montmorillonite nanocomposites: Preparation and characterization. *Polymer*
10 *Degradation and Stability*. **90**,123 (2005).
11
12 [16] M. Darder, M. Colilla, E. Ruiz-Hitzky. Biopolymer-Clay Nanocomposites Based on
13 Chitosan Intercalated in Montmorillonite. *Chemistry of Materials*. **15**,3774 (2003).
14
15 [17] M. Darder, M. Colilla, E. Ruiz-Hitzky. Chitosan-clay nanocomposites: application as
16 electrochemical sensors. *Applied Clay Science*. **28**,199 (2005).
17
18 [18] J. Labille, F. Thomas, I. Bihannic, C. Santaella. Destabilization of montmorillonite
19 suspensions by Ca²⁺ and succinoglycan. *Clay Minerals*. **38**,173 (2003).
20
21 [19] N. Amellal, G. Burtin, F. Bartoli, T. Heulin. Colonization of wheat roots by an
22 exopolysaccharide-producing *Pantoea agglomerans* strain and its effect on rhizosphere soil
23 aggregation. *Applied and Environmental Microbiology*. **64**,3740 (1998).
24
25 [20] C. Chenu, J. Guerif. Mechanical strength of clay minerals as influenced by an adsorbed
26 polysaccharide. *Soil Science Society of America Journal*. **55**,1076 (1991).
27
28 [21] C. Chenu. Influence of a fungal polysaccharide, scleroglucan, on clay microstructures.
29 *Soil Biology & Biochemistry*. **21**,299 (1989).
30
31 [22] K. M. Dontsova, J. M. Bigham. Anionic polysaccharide sorption by clay minerals. *Soil*
32 *Science Society of America Journal*. **69**,1026 (2005).
33
34 [23] M. He, Y. Horikawa. Partial deflocculation of mutual flocs of allophane and halloysite
35 by xanthan and chitosan and relevance to particle arrangement in the flocs. *Soil Science and*
36 *Plant Nutrition (Tokyo)*. **46**,81 (2000).
37
38 [24] S. M. Rao, A. Sridharan, M. R. Shenoy. Influence of starch polysaccharide on the
39 remolded properties of two Indian clay samples. *Canadian Geotechnical Journal*. **30**,550
40 (1993).
41
42 [25] A. Olness, C. E. Clapp. Occurrence of collapsed and expanded crystals in
43 montmorillonite-dextran complexes. *Clays and Clay Minerals, Proceedings of the*
44 *Conference*. **21**,289 (1973).
45
46 [26] J. Labille, F. Thomas, M. Milas, C. Vanhaverbeke. Flocculation of colloidal clay by
47 bacterial polysaccharides: effect of macromolecule charge and structure. *Journal of Colloid*
48 *and Interface Science*. **284**,149 (2005).
49
50
51
52
53
54
55
56
57
58
59
60

- 1
2
3 [27] S. I. Tsipursky, V. A. Drits. The distribution of octahedral cations in the 2:1 layers of
4 dioctahedral smectites studied by oblique-texture electron diffraction. *Clay Minerals*. **19**,177
5 (1984).
6
7
8 [28] P. Capkova, M. Pospisil, M. Valaskova, D. Merinska, M. Trchova, Z. Sedlakova, Z.
9 Weiss, J. Simonik. Structure of montmorillonite cointercalated with stearic acid and
10 octadecylamine: Modeling, diffraction, IR spectroscopy. *Journal of Colloid and Interface*
11 *Science*. **300**,264 (2006).
12
13 [29] A. Gaudel-Siri, P. Brocorens, D. Siri, F. Gardebien, J.-L. Bredas, R. Lazzaroni.
14 Molecular Dynamics Study of e-Caprolactone Intercalated in Wyoming Sodium
15 Montmorillonite. *Langmuir*. **19**,8287 (2003).
16
17 [30] P. Capkova, P. Maly, M. Pospisil, Z. Klika, H. Weissmannova, Z. Weiss. Effect of
18 surface and interlayer structure on the fluorescence of rhodamine B-montmorillonite:
19 modeling and experiment. *Journal of Colloid and Interface Science*. **277**,128 (2004).
20
21 [31] M. Fermeglia, M. Ferrone, S. Pricl. Computer simulation of nylon-6/organoclay
22 nanocomposites: prediction of the binding energy. *Fluid Phase Equilibria*. **212**,315 (2003).
23
24 [32] P. Capkova, J. V. Burda, Z. Weiss, H. Schenk. Modeling of aniline-vermiculite and
25 tetramethylammonium-vermiculite; test of force fields. *Journal of Molecular Modeling*. **5**,8
26 (1999).
27
28 [33] S. Perez, M. Kouwijzer, K. Mazeau, S. B. Engelsen. Modeling polysaccharides: present
29 status and challenges. *Journal of Molecular Graphics*. **14**,307 (1996).
30
31 [34] C. Vanhaverbeke, A. Heyraud, K. Mazeau. Conformational analysis of the
32 exopolysaccharide from *Burkholderia caribensis* strain MWAP71: Impact on the interaction
33 with soils. *Biopolymers*. **69**,480 (2003).
34
35 [35] A. K. Rappe, C. J. Casewit, K. S. Colwell, W. A. Goddard, III, W. M. Skiff. UFF, a full
36 periodic table force field for molecular mechanics and molecular dynamics simulations.
37 *Journal of the American Chemical Society*. **114**,10024 (1992).
38
39 [36] R. Toth, A. Coslanich, M. Ferrone, M. Fermeglia, S. Pricl, S. Miertus, E. Chiellini.
40 Computer simulation of polypropylene/organoclay nanocomposites: characterization of
41 atomic scale structure and prediction of binding energy. *Polymer*. **45**,8075 (2004).
42
43 [37] F. Gardebien, J.-L. Bredas, R. Lazzaroni. Molecular dynamics simulations of
44 nanocomposites based on poly(e-caprolactone) grafted on montmorillonite clay. *Journal of*
45 *Physical Chemistry B*. **109**,12287 (2005).
46
47 [38] A. K. Rappe, W. A. Goddard, III. Charge equilibration for molecular dynamics
48 simulations. *Journal of Physical Chemistry*. **95**,3358 (1991).
49
50
51
52
53
54
55
56
57
58
59
60

- 1
2
3 [39] H. Q. Ding, N. Karasawa, W. A. Goddard, III. Atomic level simulations on a million
4 particles: the cell-multipole method for Coulomb and London nonbond interactions. *Journal*
5 *of Chemical Physics*. **97**,4309 (1992).
6
7
8 [40] L. Verlet. Computer \"experiments\" on classical fluids. I. Thermodynamical properties
9 of Lennard-Jones molecules. *Physical Review*. **159**,98 (1967).
10
11 [41] D. J. Evans, B. L. Holian. The Nose-Hoover thermostat. *Journal of Chemical Physics*.
12 **83**,4069 (1985).
13
14 [42] M. L. Connolly. Computation of molecular volume. *Journal of the American Chemical*
15 *Society*. **107**,1118 (1985).
16
17 [43] L. G. Fuller, T. B. Goh, D. W. Oscarson, C. G. Biliaderis. Flocculation and coagulation
18 of Ca- and Mg-saturated montmorillonite in the presence of a neutral polysaccharide. *Clays*
19 *and Clay Minerals*. **43**,533 (1995).
20
21 [44] Y. M. Kanaani, A. Adin, C. Rav-Acha. Biofilm interactions in water reuse systems:
22 adsorption of polysaccharide to kaolin. *Water Science and Technology*. **26**,673 (1992).
23
24 [45] B. Gu, H. E. Doner. The interaction of polysaccharides with Silver Hill illite. *Clays and*
25 *Clay Minerals*. **40**,151 (1992).
26
27 [46] A. J. Simpson, M. J. Simpson, W. L. Kingery, B. A. Lefebvre, A. Moser, A. J. Williams,
28 M. Kvasha, B. P. Kelleher. The application of ¹H high-resolution magic-angle spinning NMR
29 for the study of clay-organic associations in natural and synthetic complexes. *Langmuir*.
30 **22**,4498 (2006).
31
32 [47] K. D. Kwon, H. Green, P. Bjoern, J. D. Kubicki. Model Bacterial Extracellular
33 Polysaccharide Adsorption onto Silica and Alumina: Quartz Crystal Microbalance with
34 Dissipation Monitoring of Dextran Adsorption. *Environmental Science & Technology*.
35 **40**,7739 (2006).
36
37
38
39
40
41
42
43
44
45
46
47
48
49
50
51
52
53
54
55
56
57
58
59
60